

Supporting Information

Self-assembly of high-nuclear core-shell polyoxovanadates with Lindqvist templates

Shuangxue Wu,^a Yaomei Fu,^b Hongmei Gan,^a Liang Zhao,^{*a} Xinlong Wang,^a Chao Qin^{*a} and Zhongmin Su^c

^aKey Laboratory of Polyoxometalate and Reticular Material Chemistry of Ministry of Education, Northeast Normal University, Changchun, Jilin 130024.

^bShandong Peninsula Engineering Research Center of Comprehensive Brine Utilization, Weifang University of Science and Technology, Shouguang 262700, China.

^cKey Laboratory of Advanced Materials of Tropical Island Resources, Hainan University, Haikou 570228, China.

*Corresponding Authors: zhaol352@nenu.edu.cn; qinc703@nenu.edu.cn

Experimental Procedures

Materials and methods

VOSO₄·xH₂O, Na₂WO₄·4H₂O, Na₂MoO₄·6H₂O, Bi(NO₃)₃·6H₂O, Cu(NO₃)₂·6H₂O, Phenylphosphonic acid, and sulfur oxide were purchased from Aladdin commercial companies. Acetonitrile, methanol, N, N-Dimethylformamide, ethylenediamine, and 30% H₂O₂ were obtained from Tianjin Fuyu Fine Chemical Co., Ltd., and all commercial reagents and solvents were used without further purification.

Single-crystal X-ray diffraction data for the **1** and **2** were recorded using a Germany Bruker D8 VENTURE diffractometer with graphite-monochromated Cu K α radiation ($\lambda = 0.15406$ nm) at 298.02 K. SADABS software was used for multiscan absorption corrections. The crystal structures were solved via the direct method and refined using full-matrix methods against F^2 from the SHELXTL package and Olex 2 software. Anisotropic refinement was performed for all non-hydrogen atoms. The restrained DFIX, SIMU, ISOR instructions were used to make the structures more reasonable. The solvent molecules and counterions in **1** and **2** are disordered, hindering the modeling of the crystal structure. Therefore, all guest molecules and counterions in **1** and **2** were removed using the SQUEEZE option of PLATON. The specific crystallographic data and structure refinement results of the compound **1** and **2** are shown in Table S1. Crystallographic data from **1** and **2** were delivered to the Cambridge Crystallographic Data Centre (CCDC) and assigned No. 2401866 and 2401867.

Powder X-ray diffraction (PXRD) patterns were measured with a Smartlab diffractometer, radiating through Cu K α ($\lambda = 0.15418$ nm) in the range 5°–50° at a rate of 10° min⁻¹. Thermogravimetric analysis was measured with a Japan DTG-60H thermogravimetric differential thermal analyzer under a nitrogen atmosphere, heated at a rate of 10° min⁻¹ from room temperature to 4000 °C. Infrared spectra were measured using the KBr press method on a Cary 7000 FT/IR spectrophotometer in the range of 4000–400 cm⁻¹. X-ray photoelectron spectroscopy (XPS) was carried out using an XPS system (Thermo-Fisher, ESCLAB 250, USA).

Results and Discussion

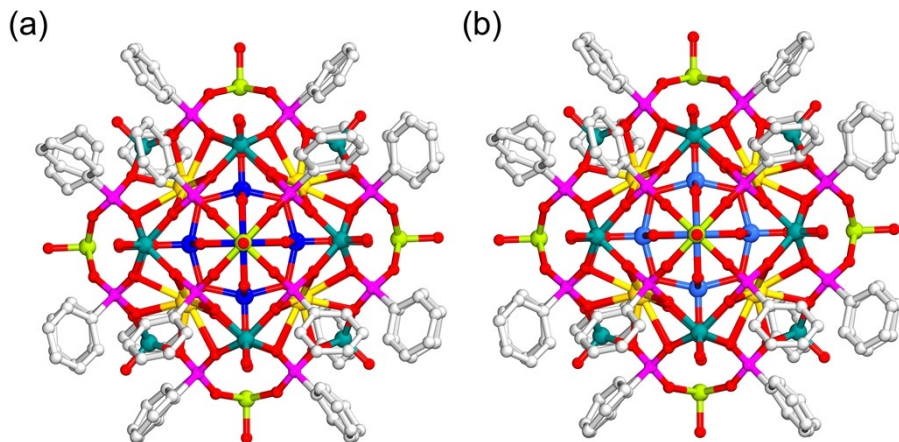


Figure S1. (a) and (b) Ball-and-stick modeling compounds **1** and **2**, respectively. Color code: red, O; pink, P; yellow, Na; green, V; blue, W; light blue, Mo. H atoms are omitted for clarity.

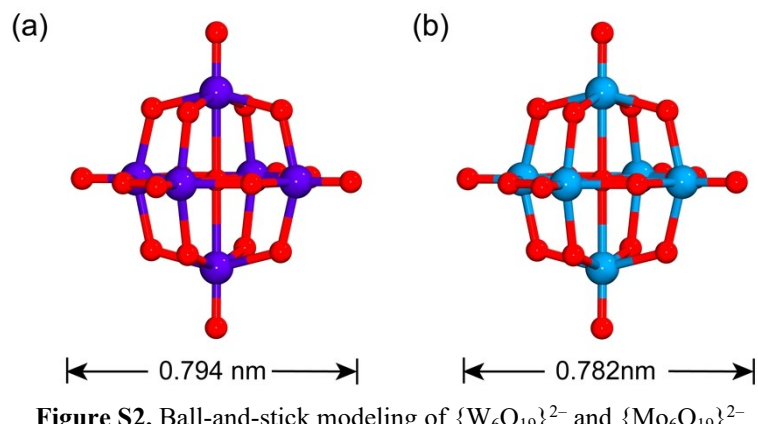


Figure S2. Ball-and-stick modeling of $\{W_6O_{19}\}^{2-}$ and $\{Mo_6O_{19}\}^{2-}$

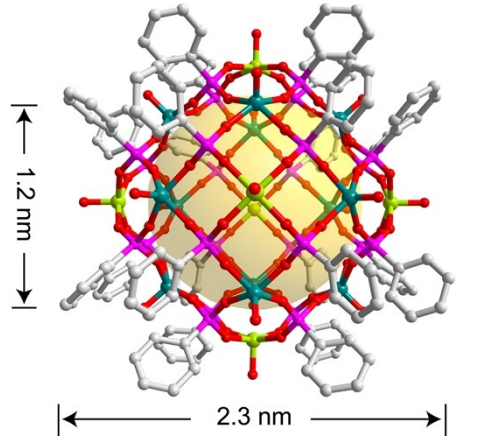


Figure S3. Ball-and-stick model for shell $\{V^V_6V^{IV}_{12}O_{18}(PhPO_3)_{24}\}^{6-}$. Color code: red, O; pink, P; green, V. H atoms are omitted for clarity.

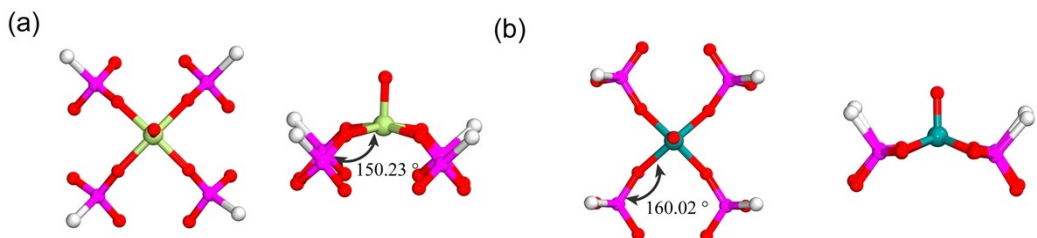


Figure S4. (a) and (b) Top and main views of the square pyramids $\{\text{V}^{\text{V}}\text{O}_5(\text{PhPO}_3)_4\}$ and $\{\text{V}^{\text{IV}}\text{O}_5(\text{PhPO}_3)_4\}$, respectively.

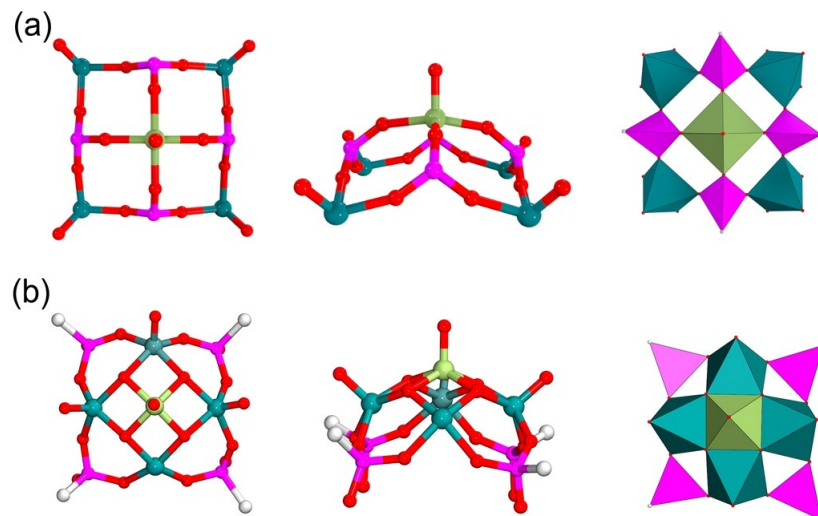


Figure S5. (a) and (b) Ball-and-stick models and polyhedral diagrams of $\{\text{V}^{\text{V}}\text{V}^{\text{IV}}_4(\text{PhPO}_3)_4\}$ and $\{\text{V}_5\text{P}_4\}$, respectively.

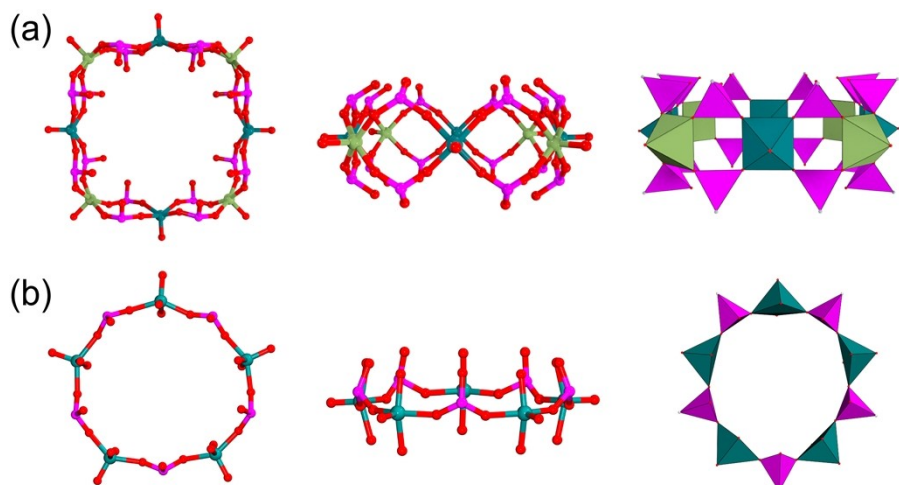


Figure S6. (a) and (b) Ball-and-stick models and polyhedral diagrams of $\{\text{V}^{\text{V}}_4\text{V}^{\text{IV}}_4(\text{PhPO}_3)_{16}\}$ and $\{\text{V}^{\text{V}}\text{O}_5(\text{PhPO}_3)_4\}$, respectively.

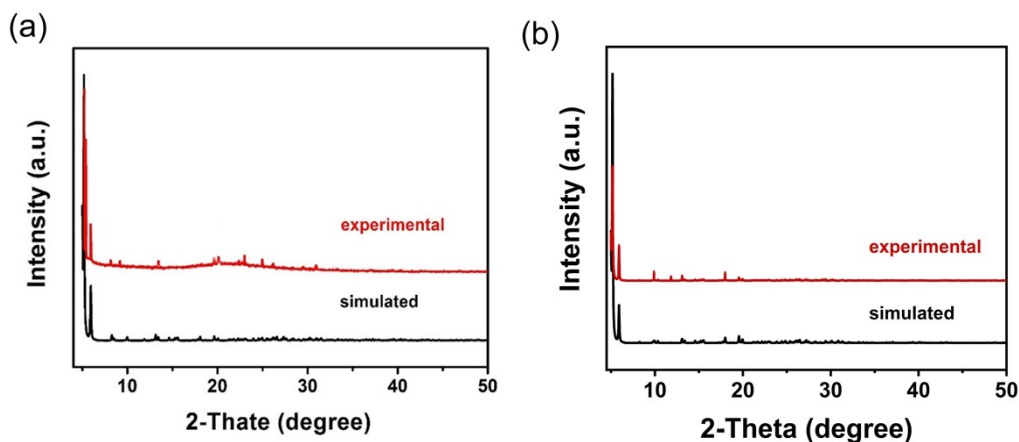


Figure S7. (a) and (b) Experimental and simulated powder X-ray diffraction patterns for compounds **1** and **2**, respectively.

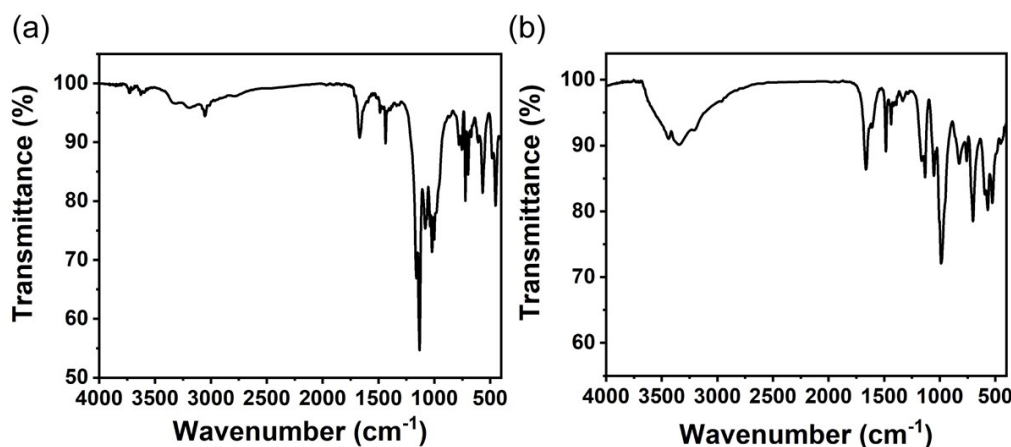


Figure S8. (a) and (b) Fourier transform infrared (FTIR) spectra of compounds **1** and **2**, respectively.

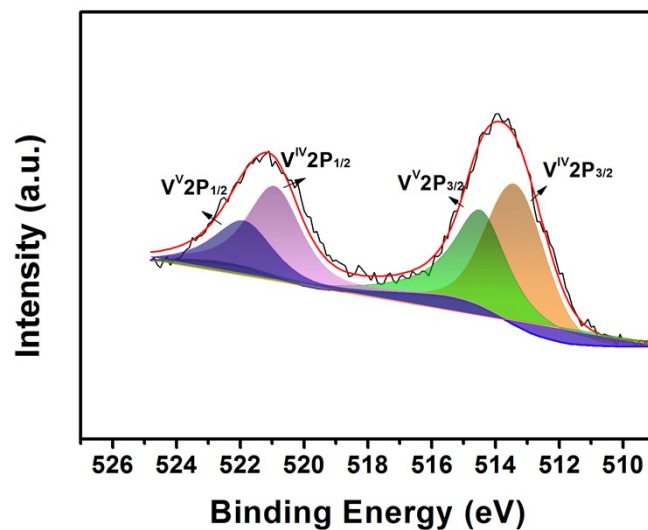


Figure S9. XPS spectra of compound **1** for V 2p_{3/2} and V 2p_{1/2}.

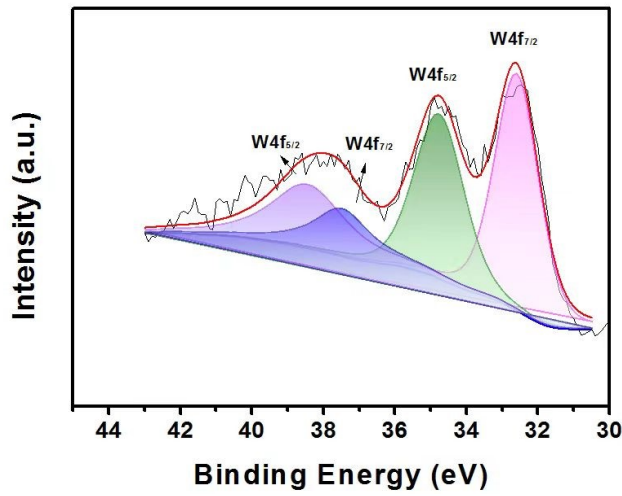


Figure S10. XPS spectra of compound **1** for W 4f_{5/2} and W 4f_{7/2}.

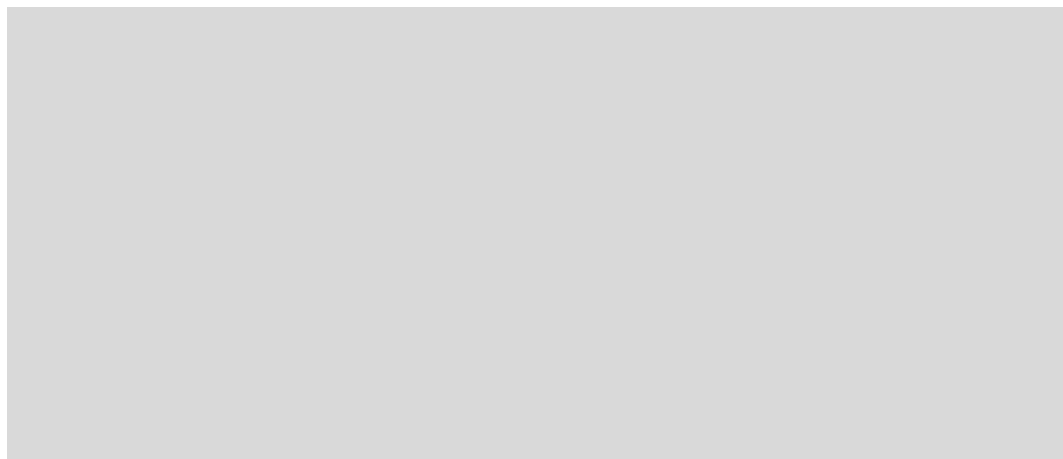


Figure S11. (a) and (b) Thermogravimetric analytical traces of compounds **1** and **2**, respectively.

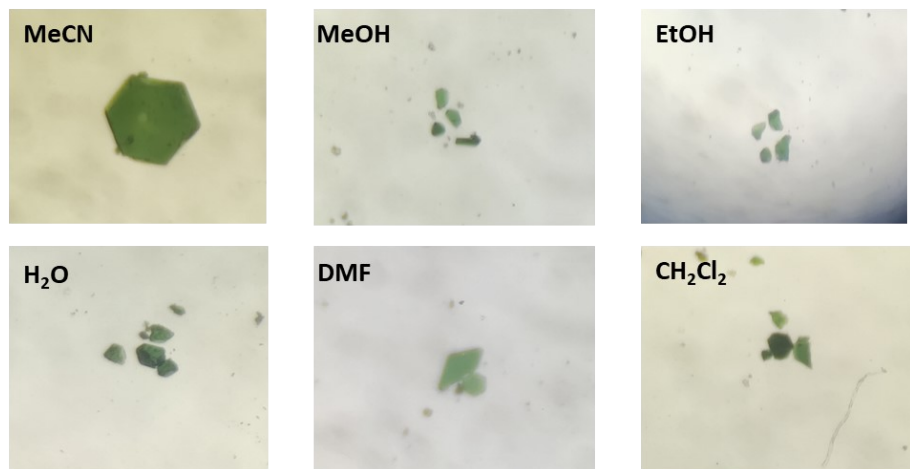


Figure S12. Photograph of crystal **1** after 3 days of immersion in different solvents.

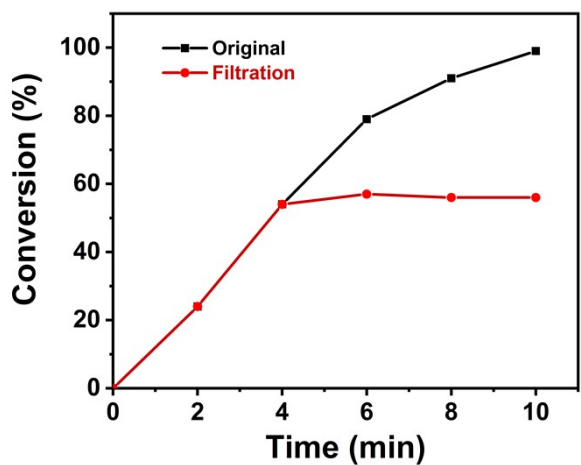


Fig. S13 Dynamic conversion curve of methyl phenyl sulfide catalyzed by compound **1** (black), and the catalyst was filtered out at 4 min of the reaction (red).

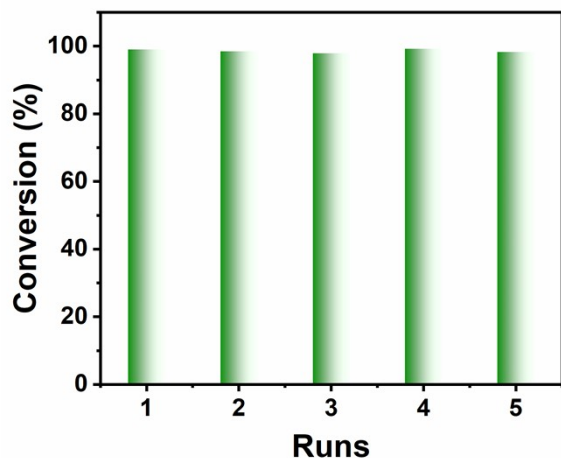


Fig. S14 Circular experimental diagram of methyl phenyl sulfide catalyzed by compound **1**.

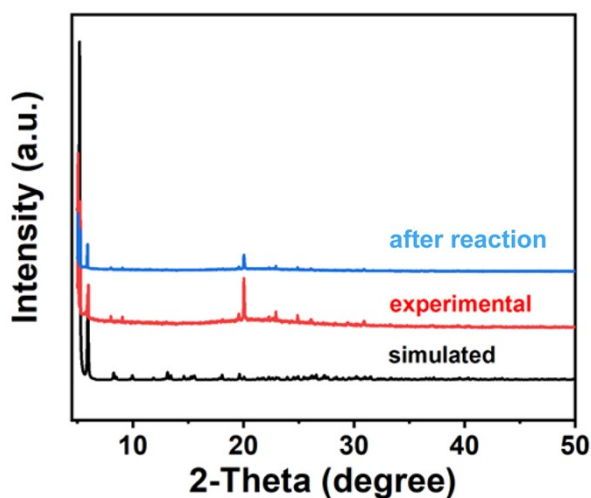


Fig. S15 The PXRD patterns for **1**: simulated (black), experimental (red), after recycle (blue).

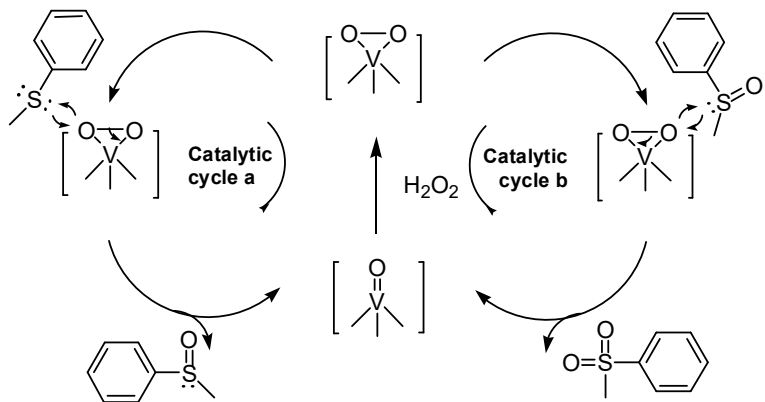


Figure S16. Possible mechanism for the catalysis of methyl phenyl sulphide (MBT) by compound **1**. We conducted a control experiment utilizing phenylphosphonic acid and $[W_6O_{19}]^{2-}$, which exhibited a minimal catalytic influence on MBT, indicating that vanadate serves as the primary active species. Based on the reported literature related to the catalytic oxidation of POVs¹⁻⁸, we propose a possible mechanism for the catalytic oxidation of MBT by compound **1**. The V atom in the $\{VO_5\}$ moiety of compound **1** was oxidised by H_2O_2 to vanadium peroxide, which was subsequently attacked by the S atom in MBT to give the sulfoxide. The sulfoxide is further attacked nucleophilically by vanadium peroxide to give the final product sulfone.

Table S1. Crystallographic data for compounds **1** and **2**

Compound	1	2
Empirical formula	$C_{144}H_{120}Na_8O_{109}P_{24}V_{18}W_6$	$C_{144}H_{120}Na_8O_{109}P_{24}V_{18}Mo_6$
Formula weight	6919.2	5992.4
Temperature/K	284.28	293(2)
Crystal system	trigonal	trigonal
Space group	<i>R</i> -3	<i>R</i> -3
<i>a</i> /Å	20.772(4)	20.8705(5)
<i>b</i> /Å	20.772(4)	20.8705(5)
<i>c</i> /Å	53.061(19)	53.328(3)
$\alpha/^\circ$	90	90
$\beta/^\circ$	90	90
$\gamma/^\circ$	120	120
Volume/Å ³	19827(10)	20116.5(14)
<i>Z</i>	3	3
ρ_{calcd}/cm^3	1.664	1.564
<i>F</i> (000)	9486.0	9165.0
Reflections collected	32591	21350
Independent reflections	7360	4684
<i>R</i> int	0.0338	0.0417
Goodness-of-fit on <i>F</i> ²	1.087	1.072
Final <i>R</i> indexes [$I >= 2\sigma(I)$]	$R_I = 0.1257$, $wR_2 = 0.2834$	$R_I = 0.0748$, $wR_2 = 0.2078$
Final <i>R</i> indexes [all data]	$R_I = 0.1315$, $wR_2 = 0.2861$	$R_I = 0.0868$, $wR_2 = 0.2168$
$R_I = F_o - F_c / F_o $, $wR_2 = \sqrt{w(F_o^2 - F_c^2)^2/w(F_o^2)^2}$		

Table S2. Bond lengths for compound 1.

Atom	Atom	Length/Å	Atom	Atom	Length/Å
W1	O1	2.3235(10)	O1	W2 ⁵	2.351(9)
W1	O2	1.586(13)	O1	W2 ²	2.351(9)
C19b	C20	1.35(11)	O1	W2 ⁴	2.351(9)
C21b	C22	1.38(11)	O1	W2	2.351(9)
C22b	C23	1.392(18)	O1	W2 ³	2.351(9)
C19b	C23	1.392(18)	O1	W2 ¹	2.351(9)
C24a	C25	1.39	O2	W2	1.971(16)
C20b	C26	1.390(18)	O3	Na1	2.486(18)
C25a	C26	1.39	O5	Na2	2.73(2)
C21b	C26	1.390(18)	O6	V1 ²	1.952(16)
C27a	C28	1.39	O6	Na1	2.58(2)
W1	O18 ¹	1.931(11)	O7	Na1	2.65(2)
W1	O18	1.921(11)	O8	Na1	2.56(2)
W1	O19 ²	1.929(11)	O10	V2 ¹	1.943(16)
W1	O19	1.943(11)	O10	Na2	2.65(2)
W1	Na1 ³	3.552(8)	O11	V3 ⁴	2.09(2)
W1	Na1	3.537(7)	O13	V1 ²	1.893(15)
W1	Na2	3.542(12)	O13	Na1	2.75(2)
W1	W2	0.935(9)	C1	C2	1.42(3)
W1	W2 ³	2.900(9)	C1	C10	1.33(3)
W1	W2 ⁴	2.731(9)	O14	V3 ³	1.935(19)
V1	O3	2.07(2)	O16	Na1	2.62(2)
V1	O6 ³	1.952(16)	C2	C11	1.42(3)
V1	O8	1.921(15)	C3	C4	1.39
V1	O9	1.606(14)	C3	C8	1.39
V1	O13 ³	1.893(15)	C4	C5	1.39
V1	Na1	3.498(9)	C5	C6	1.39
V1	Na1 ³	3.582(8)	C6	C7	1.39
V2	O5	1.904(19)	C7	C8	1.39
V2	O7	1.937(16)	C9	C11	1.31(3)
V2	O10 ⁴	1.943(16)	C9	C18	1.31(3)
V2	O12	1.544(15)	C10	C18	1.46(3)
V2	O16	1.942(19)	C12	C13	1.39
V2	Na1	3.586(9)	C12	C17	1.39
V2	Na2	3.574(4)	C13	C14	1.39
V3	O4	1.625(13)	C14	C15	1.39
V3	O11 ¹	2.09(2)	C15	C16	1.39
V3	O14 ²	1.935(19)	C16	C17	1.39
V3	O15	1.89(2)	C23	C24	1.39
V3	O17	1.94(2)	C23	C28	1.39
P1	O3	1.36(2)	C26	C27	1.39

P1	O13	1.493(16)	O18	W1 ⁴	1.932(11)	
P1	C1	1.79(2)	O18	Na1 ⁴	2.641(13)	
P1	O14	1.424(19)	O18	Na2	2.680(16)	
P1	Na1	3.219(9)	O18	W2 ⁴	1.274(15)	
P2	O8	1.496(17)	O19	W1 ³	1.929(11)	
P2	O11	1.34(2)	O19	Na1 ⁴	2.687(14)	
P2	O16	1.47(2)	O19	Na1 ³	2.632(14)	
P2	C12	1.774(12)	O19	W2 ³	1.555(14)	
P2	Na1	3.215(9)	Na1	O18 ¹	2.641(13)	
P3	O6	1.449(16)	Na1	O19 ²	2.632(14)	
P3	O7	1.463(18)	Na1	O19 ¹	2.687(14)	
P3	C3	1.800(11)	Na1	W2	2.653(12)	
P3	O17	1.43(2)	Na2	P4 ⁴	3.220(8)	
P3	Na1	3.203(9)	Na2	P4 ¹	3.220(8)	
P4	O5	1.470(19)	Na2	O5 ¹	2.73(2)	
P4	O10	1.434(17)	Na2	O5 ⁴	2.73(2)	
P4	O15	1.46(2)	Na2	O10 ¹	2.65(2)	
P4	C23	1.781(16)	Na2	O10 ⁴	2.65(2)	
P4	Na2	3.220(8)	Na2	O18 ¹	2.680(16)	
O1	W1 ⁵	2.3233(10)	Na2	O18 ⁴	2.680(16)	
O1	W1 ³	2.3232(10)	W2	W1 ¹	2.731(9)	
O1	W1 ⁴	2.3233(10)	W2	W1 ²	2.900(9)	
O1	W1 ¹	2.3233(10)	W2	O18 ¹	1.273(15)	
O1	W1 ²	2.3232(10)	□	W2	O19 ²	1.555(14)

¹+Y-X,1-X,+Z; ²-1/3+Y,1/3-X+Y,4/3-Z; ³2/3-Y+X,1/3+X,4/3-Z; ⁴1-Y,1+X-Y,+Z; ⁵2/3-X,4/3-Y,4/3-Z

Table S3. Bond lengths for compound 2.

Atom	Atom	Length/Å	□	Atom	Atom	Length/Å
Mo1	O1	2.3380(7)		O3	Na1 ³	2.647(9)
Mo1	O2	1.635(10)		O3	Na1	2.667(9)
Mo1	O3	1.945(7)		O4	Mo1 ⁴	1.939(7)
Mo1	O3 ¹	1.938(7)		O4	Na1 ³	2.667(10)
Mo1	O4 ²	1.939(7)		O4	Na2	2.647(11)
Mo1	O4	1.946(7)		O5	Na1	2.575(12)
C14a	C15	1.39		O6	Na1 ³	2.680(12)
C15a	C16	1.39		O7	V1 ³	1.941(10)
C17a	C18	1.39		O7	Na1 ³	2.610(12)
Mo1	Na1 ¹	3.558(5)		O8	V1 ⁴	1.936(10)
Mo1	Na1	3.552(5)		O8	Na1 ³	2.581(13)
Mo1	Na1 ³	3.541(5)		O9	V2 ²	1.949(10)
Mo1	Na2	3.557(8)		O9	Na2	2.651(13)
C25b	C27	1.374(15)		O11	Na2	2.621(12)
C26b	C28	1.387(15)		O13	V1 ³	1.932(9)

V1	O5	1.944(9)	O13	Na1	2.766(15)
V1	O7 ¹	1.941(10)	O15	Na1 ³	2.680(15)
V1	O8 ²	1.936(10)	C1	C6	1.390(19)
V1	O10	1.572(9)	C1	C10	1.41(2)
V1	O13 ¹	1.932(9)	C2	C8	1.41(2)
V1	Na1 ¹	3.585(5)	C2	C22	1.37(2)
V1	Na1	3.533(5)	O18	V3 ⁴	1.932(10)
V2	O6	1.908(9)	C3	C7	1.37(2)
V2	O9 ⁴	1.949(10)	C3	C9	1.38(2)
V2	O11	1.945(10)	C4	C5	1.38(2)
V2	O12	1.590(9)	C4	C6	1.358(19)
V2	O15	1.925(11)	C5	C12	1.32(2)
V2	Na1 ³	3.602(5)	C7	C11	1.40(2)
V2	Na2	3.594(3)	C8	C19	1.35(2)
V3	O14	1.721(9)	C9	C23	1.36(2)
V3	O16	1.926(10)	C10	C12	1.40(2)
V3	O17	1.915(10)	C11	C21	1.30(2)
V3	O18 ²	1.932(10)	C13	C14	1.39
V3	O19	1.903(10)	C13	C18	1.39
P1	O5	1.477(10)	C13	C25	1.384(15)
P1	O13	1.475(10)	C13	C26	1.391(15)
P1	C1	1.773(14)	C16	C17	1.39
P1	O19	1.461(11)	C16	C27	1.386(15)
P1	Na1	3.262(6)	C16	C28	1.396(15)
P2	O6	1.502(10)	C19	C20	1.29(2)
P2	O8	1.473(10)	C20	C24	1.35(2)
P2	O18	1.449(11)	C21	C23	1.34(2)
P2	C3	1.784(13)	C22	C24	1.41(2)
P2	Na1 ³	3.222(6)	Na1	P2 ¹	3.222(6)
P3	O7	1.489(9)	Na1	P3 ¹	3.243(6)
P3	O15	1.489(11)	Na1	O3 ¹	2.647(9)
P3	O16	1.457(10)	Na1	O4 ¹	2.668(10)
P3	C2	1.773(15)	Na1	O6 ¹	2.680(12)
P3	Na1 ³	3.243(6)	Na1	O7 ¹	2.610(12)
P4	O9	1.483(10)	Na1	O8 ¹	2.581(13)
P4	O11	1.480(10)	Na1	O15 ¹	2.680(15)
P4	O17	1.455(11)	Na2	P4 ⁴	3.253(5)
P4	C13	1.786(12)	Na2	P4 ²	3.253(5)
P4	Na2	3.253(5)	Na2	O4 ⁴	2.647(11)
O1	Mo1 ⁴	2.3379(7)	Na2	O4 ²	2.647(11)
O1	Mo1 ²	2.3379(7)	Na2	O9 ²	2.651(13)
O1	Mo1 ⁵	2.3380(7)	Na2	O9 ⁴	2.651(13)
O1	Mo1 ¹	2.3380(7)	Na2	O11 ²	2.621(12)
O1	Mo1 ³	2.3379(7)	Na2	O11 ⁴	2.621(12)

O3	Mol ³	1.938(7)	□	□	□	□
		$^1_{-1/3+Y,1/3-X+Y,4/3-Z}; ^2_{+Y-X,1-X,+Z}; ^3_{2/3-Y+X,1/3+X,4/3-Z}; ^4_{1-Y,1+X-Y,+Z}; ^5_{2/3-X,4/3-Y,4/3-Z}$				

Table S4. Selected Angles [deg] for Compound **1**

Atom	Atom	Atom	Angle/ [°]	□	Atom	Atom	Atom	Angle/ [°]
O2	W1	O18 ³	103.9(6)		V1	O8	Na1	101.7(8)
C28a	C27a	C26	120		P2	O8	V1	156.6(13)
C22b	C21b	C26	114(6)		P2	O8	Na1	101.7(9)
O2	W1	O18	104.3(6)		V2 ³	O10	Na2	101.0(8)
O2	W1	O19 ⁴	102.1(6)		P4	O10	V2 ³	159.1(16)
O2	W1	O19	103.0(6)		P4	O10	Na2	99.7(10)
O2	W1	Na1 ¹	86.3(5)		P2	O11	V3 ²	147.0(12)
O2	W1	Na1	86.2(5)		V1 ⁴	O13	Na1	99.4(8)
O2	W1	Na2	87.8(5)		P1	O13	V1 ⁴	165.1(17)
O2	W1	W2 ¹	127.6(5)		P1	O13	Na1	94.1(9)
O2	W1	W2 ²	126.0(5)		C2	C1	P1	119.5(18)
O18 ³	W1	O1	76.3(4)		C10	C1	P1	123.1(16)
O18	W1	O1	76.5(4)		C10	C1	C2	117(2)
O18	W1	O18 ³	88.4(6)		P1	O14	V3 ¹	153.9(13)
O18	W1	O19 ⁴	153.6(5)		P4	O15	V3	156.4(12)
O7	V2	O10 ²	147.1(8)		O8	Na1	O6	140.9(6)
O7	V2	O16	80.9(11)	□	O8	Na1	O7	107.8(6)

Table S5. Selected Angles [deg] for Compound **2**

Atom	Atom	Atom	Angle/ [°]	□	Atom	Atom	Atom	Angle/ [°]
O1	Mol	Na1 ¹	92.99(8)		P2	O6	Na1 ¹	96.7(5)
C28b	C26b	C13	115(3)		V1 ¹	O7	Na1 ¹	100.8(4)
O1	Mol	Na1 ²	92.56(8)		P3	O7	V1 ¹	158.0(7)
C27b	C25b	C13	123(3)		P3	O7	Na1 ¹	101.0(5)
C17a	C18a	C13	120		V1 ⁴	O8	Na1 ¹	104.1(5)
O1	Mol	Na1	92.70(9)		P2	O8	V1 ⁴	153.1(8)
O1	Mol	Na2	92.78(8)		P2	O8	Na1 ¹	101.8(6)
O2	Mol	O1	179.8(3)		V2 ³	O9	Na2	101.7(5)
O2	Mol	O3 ²	103.4(4)		P4	O9	V2 ³	158.1(9)
O2	Mol	O3	103.2(4)		P4	O9	Na2	100.0(6)
O2	Mol	O4	103.3(4)		V2	O11	Na2	102.8(4)
C26b	C28b	C16	125(3)		P4	O11	V2	155.4(8)
O2	Mol	O4 ³	103.5(4)		P4	O11	Na2	101.3(6)
O12	V2	O11	107.5(5)		V1 ¹	O13	Na1	97.9(5)
O12	V2	O15	106.5(6)		P1	O13	V1 ¹	165.5(11)
C25b	C27b	C16	118(3)	□	P1	O13	Na1	95.7(6)

Table S6. The BVS calculations suggest the following central atom valencies for **1**

Atom	BVS calc.
W1	6.238
V1	4.208
V2	4.324
V3	4.862
P1	5.338
P2	5.026
P3	5.214
P4	5.043
Na1	1.089
Na2	1.238

Table S7. The BVS calculations suggest the following central atom valencies for **2**

Atom	BVS calc.
Mo1	5.569
V1	4.424
V2	4.271
V3	4.878
P1	5.236
P2	5.128
P3	5.144
P4	4.986
Na1	1.248
Na2	1.336

Table S8. Conversion ratio of methyl phenyl sulfide (BMT) under different conditions

Entry	Catalyst (mmol)	Oxidant	Temperature (°C)	Solvent	Time (min)	Conversion (%)	Reaction Scheme
1	0.00125	TBHP	25	MeOH	10	78.63	
2	0.00125	H2O2	25	MeOH	10	>99	

3	0.00125	H ₂ O ₂	25	MeCN	10	84.35
4	0.00125	H ₂ O ₂	25	CH ₂ Cl ₂	10	79.47
5	0.00125	H ₂ O ₂	25	H ₂ O	10	38.64
6	None	H ₂ O ₂	25	MeOH	10	19.25

Table S9. Comparison of the conversion performance of similar systems for the catalytic oxidation of methyl phenyl sulfide

Entry	Catalyst	Oxidant	Tem. (°C)	Time (min)	Con. (%)	Reference
1	{V ₂₀ W ₂ P ₂₀ }	H ₂ O ₂	25	30	>99	1
2	TBA ₂ Mo ₆ O ₁₉	H ₂ O ₂	25	180	99	2
3	Mo ₆ O ₁₉ @Pt ₆ L ₄ (NO ₃) ₁₀	H ₂ O ₂	25	180	<10	2
4	K ₆ H[V ^V ₁₇ V ^{IV} ₁₂ (OH) ₄ O ₆₀ (OOC(CH ₂) ₄ COO) ₈]·nH ₂ O	TBHP	25	60	98	3
5	[(C ₂ N ₂ H ₈) ₄ (CH ₃ O) ₄ V ^{IV} ₄ V ^V ₄ O ₁₆]·4CH ₃ OH	TBHP	40	240	100	4
6	[Co ₂ L _{0.5} V ₄ O ₁₂]·3DMF·5H ₂ O	TBHP	50	240	>99	5
7	[V ^{IV} ₈ O ₈ (CH ₃ O) ₁₆ (C ₂ O ₄)][C ₆ NH ₁₆) ₂ (CH ₃ OH) ₂	TBHP	40	240	100	6
8	(NH ₂ Me ₂) ₁₂ [(V ₅ O ₉ Cl) ₆ (L) ₈]·[MeOH] ₇	TBHP	25	60	100	7
9	[Ni(bix) ₂]{V ₄ O ₁₁ }	TBHP	25	45	100	8

Reference

- 1 T. Zhang, Y. H. Hou, B. S. Hou, L. Zhao, X. L. Wang, C. Qin and Z. M. Su, High-nuclear polyoxovanadates assembled from pentagonal building blocks, *Chem. Commun.*, 2022, **58**, 11111–11114.
- 2 C. L. Liu, M. A. Moussawi, G. Kalandia, D. E. Salazar Marcano, W. E. Shepard and T. N. Parac-Vogt, Cavity-Directed Synthesis of Labile Polyoxometalates for Catalysis in Confined Spaces, *Angew. Chem. Int. Ed.*, 2024, **63**, e202401940.
- 3 K. Wang, Y. Niu, D. Zhao, Y. Zhao, P. Ma, D. Zhang, J. Wang and J. Niu, The Polyoxovanadate-Based Carboxylate Derivative K₆H[V^V₁₇V^{IV}₁₂(OH)₄O₆₀(OOC(CH₂)₄COO)₈]·nH₂O: Synthesis, Crystal Structure, and Catalysis for Oxidation of Sulfides, *Inorg. Chem.*, 2017, **56**, 14053–14059.
- 4 J. P. Cao, Y. S. Xue, N. F. Li, J. J. Gong, R. K. Kang and Y. Xu, Lewis Acid Dominant Windmill-Shaped V₈ Clusters: A Bifunctional Heterogeneous Catalyst for CO₂ Cycloaddition and Oxidation of Sulfides, *J. Am. Chem. Soc.*, 2019, **141**, 19487–19497.
- 5 B. B. Lu, J. Yang, Y. Y. Liu and J. F. Ma, A Polyoxovanadate–Resorcin [4] arene-Based Porous Metal-Organic Framework as an Efficient Multifunctional Catalyst for the Cycloaddition of CO₂ with Epoxides and the Selective Oxidation of Sulfides, *Inorg. Chem.*, 2017, **56**, 11710–11720.
- 6 Q. D. Ping, J. P. Cao, Y. M. Han, M. X. Yang, Y. L. Hong, J. N. Li, J. L. Wang, J. L. Chen, H. Mei and Y. Xu, Eight-membered ring petal-shaped V₈ cluster: An efficient heterogeneous catalyst for selective sulfur oxidation, *Inorg. Chim. Act.*, 2021, **517**, 120198.
- 7 H. M. Gan, C. Qin, L. Zhao, C. Sun, X. L. Wang and Z. M. Su, Self-Assembled Polyoxometalate-Based Metal-Organic Polyhedra as an Effective Heterogeneous Catalyst for Oxidation of Sulfide, *Cry. Grow. Des.*, 2021, **21**, 1028–1034.
- 8 T. Y. Dang, R. H. Li, H. R. Tian, Q. Wang, Y. Lu and S. X. Liu, Tandem-like vanadium cluster chains in a polyoxovanadate-based metal-organic framework for efficient catalytic oxidation of sulfides, *Inorg. Chem. Front.*, 2021, **8**, 4367–4375.